Future of Nanocomposites

Seamus A. Curran[1,2], Shawn Liao[3], Surendra Maharjan[1,2], Alex Wang[1,2] Werner Blau[1,4], Ron Oremland[5], Marc Metcalf[1], Christopher Taylor[1], Marium Khan[1], Alex Taylor[1], Madison Du[1], Favor Akande[1], Becky Scott[5], Kenneth E. Russell[1,5]

[1]CNRG, Physics Department, Science and Research Building 1, University of Houston, Houston, TX 77204, USA

[2]Physics Department, Science and Research Building 1, University of Houston, Houston, TX 77204, USA

[3]INE., Physics Department, Science and Research Building 1, University of Houston, Houston, TX 77204, USA

[4]Physics Department, Trinity College Dublin, Dublin 2, Ireland

[4]USGS, McKelvey Build., Middlefield Road, MS 480, CA 94025, USA

[5]Barton College, School of Business & Innovation, Hines Hall, Wilson, NC 27893, USA

Abstract

Combining materials of dissimilar properties and finding successful commonalities is as old as cooking, heated vegetables that can be bland, spicy or completely different are well known. The world of metallurgy, glass making and building materials have all gone through developments where the sum of the parts is greater than the components. The notion of amalgamating two or more dissimilar materials into a resulting composite material has been studied extensively. Dating back as early as 3100 B.C., Early Dynastic Period Egyptians practiced blending straw pieces with mud to form structurally reinforced masonry units for construction.[1] Beyond what is well known as doping in semiconductors that have made Intel, Microsoft, every cell phone manufacturer daily names we are now beginning to see an emergence of new forms of doping in the form of nanocomposites. Such composite materials are generally comprised of a *filler* and a *host matrix*. The filler ordinarily imparts desirable properties and functionality to the resultant composite system while the host matrix provides a compatible

structural framework that effortlessly blends well with the filler but adds new properties what is well known as a bland material. Afterall, who would have thought that adding nanotubes to conjugated and non-conjugated plastics could have such an effect ohmically or to the EM spectrum This paper explores some of the composites that are appearing as well as now well-known bio-nanomanufacturing of rare earth materials, some of what have been patented here at the University of Houston.

Background

Micro- and macro-scaled composite materials are of unequivocal importance in modern materials science. However, these materials are ordinarily limited as a consequence of large filler size in comparison to the host matrix, large inter-filler distances, low filler density, and poor chemical reactivity between the filler and host. As the filler dimensionality approaches the nanoscale (< 100 nm), more homogeneous *nanocomposites* are realized as a consequence of higher filler densities and reactivities that yield an ensemble of inter-filler interactions. Optimization of inter-filler interactions is often manifested as physical/chemical phenomena unobserved in analogous composites with larger filler sizes.[2] As such, complementary nanocomposite design and engineering must consider all aspects of the filler, host matrix, and their interfaces/interphases.

Organic and Organosilicon-Based Host Matrices

The composition of the host matrix and the techniques utilized in nanocomposite formation are equally critical to the resultant bulk properties as the functionality of the filler(s). Macromolecules of organic monomers like propene, styrene, urethanes, acylates, glycol ethers, and carbonates assume vital roles in everyday life. Largely stemming from the overabundance of petrochemicals, organics find wide-ranging economically viable applications in contemporary materials. Notwithstanding their ubiquity, organic polymers are intrinsically susceptible to photooxidative degradation under ultraviolet

(UV) irradiation. To counteract this, additional UV stabilizers and absorbers like benzophenones and benzotriazoles are conventionally added to enhance weatherability. In addition to their commercial uses as adhesion promoters, crosslinkers, and surface modifiers, organosilanes have emerged as modular monomeric units for host matrix design in more advanced applications. This follows from their tendency to form UV-transparent siloxane-based networks upon polycondensation *via* an assortment of chemistries, yielding organically modified silicate (Ormosil) matrices.[3] The siloxane bond exhibits a significantly larger bond dissociation energy than the C-C and C-O bonds that constitute the primary chains of organic polymers. Accordingly, siloxanes typically exhibit increased thermal and chemical stability that correspond to improved weatherability.[4] While the role of organic polymers in modern materials is undoubtedly expanding, inorganic-organic hybrid materials like organosilicon compounds afford cost-effective, low temperature syntheses routes towards functionally tailorable siloxane frameworks for more robust applications.

One such synthetic approach is the sol-gel process, which involves the evolution of a colloidal solution (sol) towards a gel-like diphasic system. The reaction kinetics of the sol and morphology of the resulting gel, which can vary from dilute particles to interconnected polymeric networks, are a function of reaction conditions (e.g., time, pH, temperature, catalysts, solvents, and water content). In organo-metallic/-metalloid chemistry, sol-gel processes are typically acid- or base-catalyzed with or without additional catalysts, blocking agents, solvents, or water. The functional moieties of organosilicon compounds can include alkoxy, halogen, acrylate, acryloxy, vinyl, epoxide, isocyanate, amine, sulfhydryl, and hydroxyl groups. Such functional diversity is largely responsible for the increasing use of organosilanes in advanced applications such as self-cleaning surfaces,[5] sub-marine oil-recovery materials,[6] and laser-attenuating nonlinear optical components.[7-8]

Nanocarbon-Based Fillers

The discoveries of fullerenes, carbon nanotubes (CNTs), graphene, and their variants/derivatives between 1985 – 2004 are of seminal importance to the development of nanocarbon-based polymeric nanocomposites. These range broadly in application from high-mobility organic field-effect transistors[9-10] to flexibly-conforming electronic smart skins.[11] While very recent works have reported on exotic novel allotropes of nanometric crystalline carbon (e.g., 1D carbyne (*sp*), 2D graphyne (sp^2), 3D yne-diamond (sp-sp^3), and T-carbon),[12-14] the expansion of conjugated systems has ostensibly culminated with graphene and its derivatives. Despite its remarkable physical and chemical properties, syntheses of single-layer graphene requires intricate and exorbitant growth, deposition, and/or transfer techniques. This has largely obstructed applicational development in any concise manner outside of the semiconductor industry, where is also limited.[15-16] As an intrinsic zero-bandgap material, singe-layer graphene requires cumbersome chemical doping in electronic switching applications and, devoid of interplanar orbital overlapping and passivation effects, is particularly unstable in even mildly oxidative environments.[17] Further compounding the issue, single-layer graphene has recently been shown to exhibit nanotoxicological lysing effects (e.g., *via* unique topological edge asperities that can rupture cell walls and disrupt cellular function[18]).

Since their discovery in 1991 by Sumio Iijima,[19] with nearly a decade's worth of high-impact research amassed over graphene, CNTs and their polymorphs have contrastingly emerged as outstanding, well-rounded nanofiller candidates in nanocomposite formation. This follows largely from extensive development and successes in syntheses, processing, and scalable methodologies.[20] Refinement of state-of-the-art syntheses techniques (e.g., high-pressure carbon monoxide disproportionation (HiPCO) and plasma-enhanced catalyzed chemical vapor deposition) in the last

decade has fostered markedly improved batch-to-batch control of CNT chirality, dimensionality, morphology, yield, and defects at industrial scales. While ordered and hierarchical CNT-based polymeric nanocomposites (e.g., flexible elastomeric composites of aligned CNT arrays[21-23]) assume critical roles in advanced organic electronic materials, devices, and sensors, their elaborate synthetic procedures pose scalability challenges. Disordered CNT-based conductive polymeric nanocomposites (DCPNs) are contrastingly attractive with respect to ease-of-processability, scalability of manufacturing/syntheses techniques, and their comparatively low raw materials costs.[24]

In contrast to single-wall CNTs (SWCNTs), multi-wall CNTs (MWCNTs) afford significantly lower cost-of-manufacture, increased chemical resistance, and increased thermal stability. This has translated to myriad commercial applications including battery electrodes,[25] electromagnetic interference shielding materials,[26] radar-absorbing materials,[27] transducers,[28] organic solar cell electrodes,[29] antistatic coatings,[30] structurally/mechanically enhanced nanocomposites,[31] and water filtration membranes.[32] MWCNTs possess two or more concentrically nested nanotubules of graphene centered on a common nanotube axis that diametrically increase radially outwards. Interlayer-interactions between contiguous layers in MWCNTs yield unique phenomena such as increased tensile strength[33] and synergistic energy band contribution effects from outermost contiguous layers capable of extending to the Fermi level[34] unobserved in SWCNTs. Recent experimentally corroborated numerical models[35-36] have demonstrated the importance of maximizing the number of Fermi level-crossing energy bands (Λ) in realizing high-conductivity nanocomposites, where increasing Λ corresponds to a proportional increase in bulk conductivity, resulting from a cumulative decrease in inter-nanotube contact resistances. In comparison to metallic SWCNTs, which exhibit 2 Fermi level-crossing energy bands ($\Lambda = 2$), MWCNTs have been shown to exhibit exceptionally large Λ values ranging between 400-500.[34]

Heavy Chalcogen-Based Nanofillers

Increasing reports on the syntheses of novel allotropically diverse elemental and compound nanostructures in the literature serve as a testament to the eclectic assortment of functional nanofillers existing outside of nanocarbons. Particularly, chalcogens comprise Group 16 of the periodic table, which includes oxygen, sulfur, selenium, tellurium, polonium, and livermorium. O is typically excluded as it exhibits dissimilar chemical reactivity than the heavier chalcogens (i.e., S, Se, Te, Po, Lv). S is a nonmetallic chalcogen of notable reactivity that is vital to life and biochemical processes in the form of organosulfur compounds and metal sulfides. Moreover, both Po and Lv have found restricted/limited use as a consequence of radioactivity and short half-life (53 ms), respectively. Although continental crustal occurrences of elemental Se (~50 ppb) and Te (~1 ppb) on Earth are quite small,[37] both have found unique roles as photoconductive and photoluminescent semiconducting nanomaterials.[38-42]

Of particular interest, Te is a heavy chalcogen metalloid with unique *p*-type semiconductor behavior that exists naturally in four oxidation states (6^+, 4^+, 0, 2^-).[43-44] In distinction from S and Se, Te does not form homocyclic structures as a result of more dominant secondary bonding (e.g., interchain vdW interactions). In consideration of heightened ongoing research surrounding 2D van der Waals (vdW) and non-vdW materials, recent computational modeling efforts[45] have rekindled vigorous research interest into Te nanostructures.[46-51]

MLS10 washed cell without Cysteine HCl added

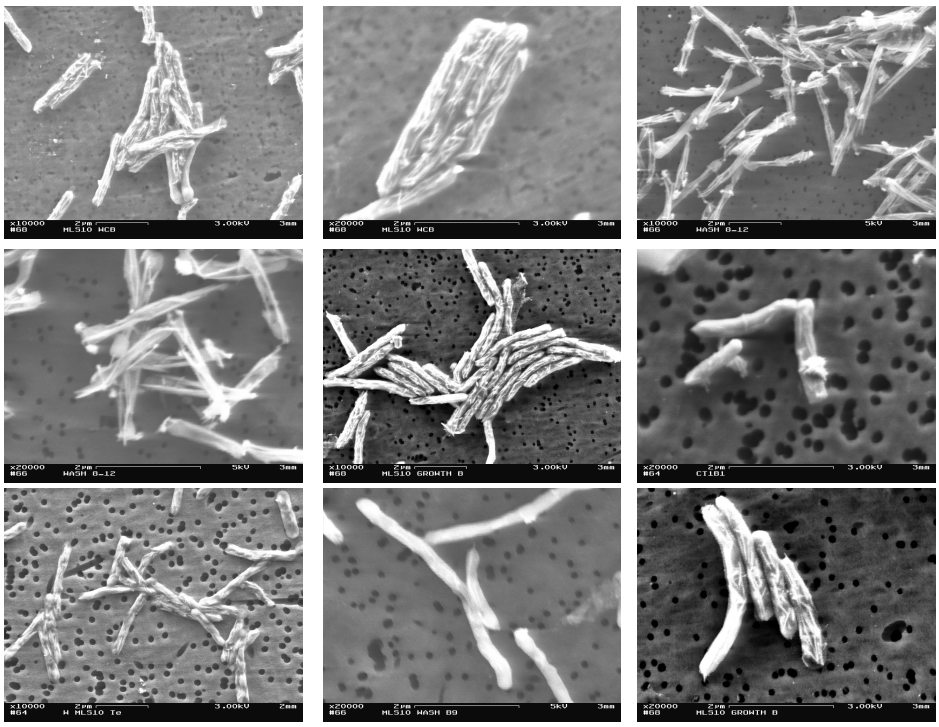

These images are from the USGS, now being made at CNRG at UH and are of bacterially respired Te nanorods which have highly unusual optical properties. This gives us a huge insight into how to for the next non-linear optical materials to beyond guiding, promises to be used against high impact lasers such as rail guns or laser targeting weaponry.

Elemental Te (Te^0) has the propensity to form 1D spiraling chains covalently-linked in an infinite helical arc of 120° parallel to its longitudinal axis (*c*-axis), where each Te atom exhibits two-fold coordination.[52-53] With remarkably small outer-chain diameters (2.35 Å),[54] isolated 1D helical Te chains are excitingly predicted to exhibit exotic topological phase transitions as well as Weyl nodes in response to applied external strain.[55-57] In 2D/3D, individual 1D helical Te chains ordinarily crystallize into a hexagonal array with an anisotropic trigonal structure *via* collective four-fold coordination interchain vdW interactions between nearest neighbors that occur across interchain distances of ~3.43 Å.[55] A synergistic combination of helically arranged intrachain antibonding orbitals and interchain interactions between lone-pair electrons result in strong molecular orbital overlap, corresponding to high carrier mobility,[49] ferroelectricity,[58] high piezoelectricity,[59] strong broadband absorption,[60] fast photoconductivity,[61-62] notable photoelectric response,[63] exceptional thermoelectric properties,[64]

excellent air-stability,[65] and unique nonlinear optical behavior.[66-68] Analogous to other vdW materials, albeit appreciably more pronounced, Te has a dimensionality- and thickness-dependent optical bandgap resulting from varying degrees of molecular orbital overlap that increases monotonically from ~0.33 eV in the bulk to ~1.2 eV for 2D atomic monolayers.[48, 69-70]

Prokaryote-Respired Chalcogen Metalloid Nanostructures

As a manifestation of strong anisotropy, the morphologies and geometries of Te nanostructures typically exhibit preferential crystal growth along the *c*-axis direction, conducive to the formation of 1D nanostructures.[71] Apart from physical techniques (e.g., chemical vapor deposition, ablation, thermal evaporation, sputtering, epitaxy, and exfoliation),[47, 49, 57, 72-73] several orthodox wet-chemical syntheses procedures largely centered on chemical/hydrothermal/solvothermal reduction of Te salts/acids (e.g., Na_2TeO_3, $Na_2TeO_4 \cdot 2H_2O$, $Te(OH)_6$)[50, 69, 74-78] as well as microwave-assisted ionic liquid reduction techniques[71, 79] have been reported on in the literature.[80] In such reduction schemes, syntheses parameters including reducing agent species, ligand/capping agent species, solvent species, molar concentrations of reagents, degree of catalytic activity, pH, temperature, pressure, and time can be combinatorically varied to yield a range of nanometric morphologies and architectures.

More recently, in stark contrast to inorganic routes, exotic *in vivo* biochemical syntheses of elemental Group VIA chalcogen (S, Se, Te) nanostructures via prokaryote-facilitated reduction of chalcogen oxyanions have been reported on in the literature that afford a distinctively innovative approach to nanoparticle syntheses.[81-90] In general, such elemental chalcogen-respiring anaerobes (e.g., *Bacillus selenitireducens*, *Sulfurospirillum barnesii*, *Thauera selenatis*, *Staphylococcus aureus*, and *Selenihalanaerobacter shriftii*)[81, 84, 87-88] utilize chalcogen oxyanions (e.g., TeO_3^{2-}, TeO_4^{2-}, SeO_3^{2-}, and SeO_4^{2-}) as electron acceptors in cellular respiratory reactions, where elemental chalcogen growth initiates both intercellularly as well as extracellularly at nucleation sites for electron transfer along the

cell wall.[91-92] Bacterially-respired elemental nanomaterials not only provide a refreshingly *green* approach to nanoparticle syntheses but also yield inimitable composite morphologies and architectures often influenced by the morphology of the bacterium cell wall itself.

Scalable High-Conductivity Multiwall Carbon Nanotube Polymeric Nanocomposites

In electronic applications, flexible nanocarbon-based DCPNs (nc-DCPNs) typically suffer from poor electrical conductivity at cost-effective loadings. This is largely attributed to extraneous and/or counterproductive carbon-nanotube processing procedures damaging to the extraordinary intrinsic physical properties of the nanotubes themselves. Mechanical and/or caustic/oxidative chemical processing methods enhance dispersibility and functionality through physical fragmentation and imparted functional moieties. However, this is to the detriment of the intrinsic electronic and phononic structures of the nanotubes *via* the introduction of physical and/or chemical defect sites that act as electron and phonon scattering centers. Ergo, a critical balance between dispersibility/functionality and preservation of the intrinsic properties of the nanotubes themselves must be maintained in pragmatic nc-DCPN design.

By significantly improving the electrical conductivity of such disordered systems using mild oxidation procedures, aqueous solvent blending techniques, and minimal mechanical processing, components of this work serve as a scalable basis upon which to expand the usage of nc-DCPNs into utilitarian applications where higher conductivities are requisite. Whereas many studies investigate the electronic transport properties of nc-DCPNs exclusively with respect to potential applications, few address pragmatic issues regarding the inimical environment in which such materials are expected to perform under that adversely affect device performance. Offsetting their excellent weatherability, fluoropolymer-based nanocomposites are cost-prohibitively application specific and find limited use in conventional applications. As such, scalable techniques for the surface modification of non-

fluorinated nc-DCPNs implementing conventional structural polymers like polyurethane (PU) to improve weatherability are of increasing importance.

The electronic and thermal responsivities of DCPN-type temperature sensing materials are an inextricable function of the convoluted interaction(s) occurring at the filler/host-matrix interface/interphase. Consequently, controlling the structure of this interfacial region is paramount towards attaining highly thermoresponsive, reproducible signals, particularly in heterogeneous amorphous systems. As temperature-sensing/thermometric materials, developmental applications of DCPNs include flexible self-healing thermal sensors,[93] thermal runaway management materials in battery safety technologies,[94] thermoresponsive transient electronic systems,[95] and implantable in vivo multi-point temperature sensing devices.[96] DCPNs in thermometric applications are typically sensitized to temperatures >100 °C and rely on solid-liquid phase changes to effectuate large-scale breakdowns of percolating conductive networks. Few systems are sensitized to human-body temperatures (~37 – 42 °C) and those that do exhibit notably poor electrical conductance at nominal operational temperatures, typically stipulating additional signal conditioning components, which are to the detriment of cost-to-manufacture. Worse yet, electrical phenomena centered on solid-liquid phase transitions impose significant device engineering challenges as form-stability issues cannot be neglected. While repeatability/reversibility of electrical phenomena in such disordered systems is typically poor, some approaches have been successful – these approaches, however, suffer from poor electrical conductivity and/or poor temperature sensitivity[(106-108)].

In an unconventional approach, this work explores the effects of tailoring the interfacial region between MWCNTs and grafted poly(octadecyl acrylate) (PODA) moieties through covalent bridging implementing a reversible addition-fragmentation chain-transfer (RAFT) polymerization scheme. Short-chain covalent bridging is demonstrated in this work to facilitate enhancements in inter-

MWCNT/PODA phononic coupling through higher-frequency non-propagating vibrational modes. Such enhancements are viable routes towards improving thermoresponsivity and repeatability of electronic phenomena in disordered systems. In doing so, subtle conformational rearrangements of covalently grafted PODA moieties at the MWCNT-PODA interface/interphase occurring across form-stable 2nd-order glass transitions are amplified. Quite remarkably, these subtle glass transitions, barely detectable through high-resolution differential thermal analysis, in coaction with covalently grafted MWCNTs, are physically manifested as the exceptionally large, temperature-dependent, repeatable/reversible temperature coefficient of resistance responses at 315 K (42 °C) observed and reported on elsewhere.

Sol-Gel Derived Transparent Ormosil-Based Ceramic Nanocomposites for Nonlinear Optical Application

A substantial body of work has been conducted regarding prokaryotic syntheses of elemental nanoparticles. However, their physical properties are disparately unexplored in comparison to those of inorganically synthesized elemental nanomaterials. While physical characterizations of novel nanomaterials are certainly of fundamental interest, pragmatic applications, outside of biomedical imaging, rarely implement isolated nanomaterials and/or their liquid-phase dispersions. As such, novel nanomaterials must consider both the properties of the active nanomaterial itself as well as dynamic interactions between the nanomaterial and respective host matrix in nanocomposite formation.[97]

In photonic and optoelectronic applications, functional nanocomposites based on organic polymer matrices are inherently susceptible to 1st- and 2nd-order phase transitions,[98] thermal decomposition,[99-100] and low damage thresholds under intense photonic irradiation, prolonged photonic irradiation, and/or in other harsh environments,[98, 101-102] severely limiting their use. It is worth noting here that the lack of research attention on optimization of transparent, robust, and

thermally/mechanically stable solid-state host matrices and their dynamic interfacial interactions with embedded nanomaterials imposes a somber bottleneck effect on the fruitful development of rational nonlinear optical and optical limiting devices.[102-103]

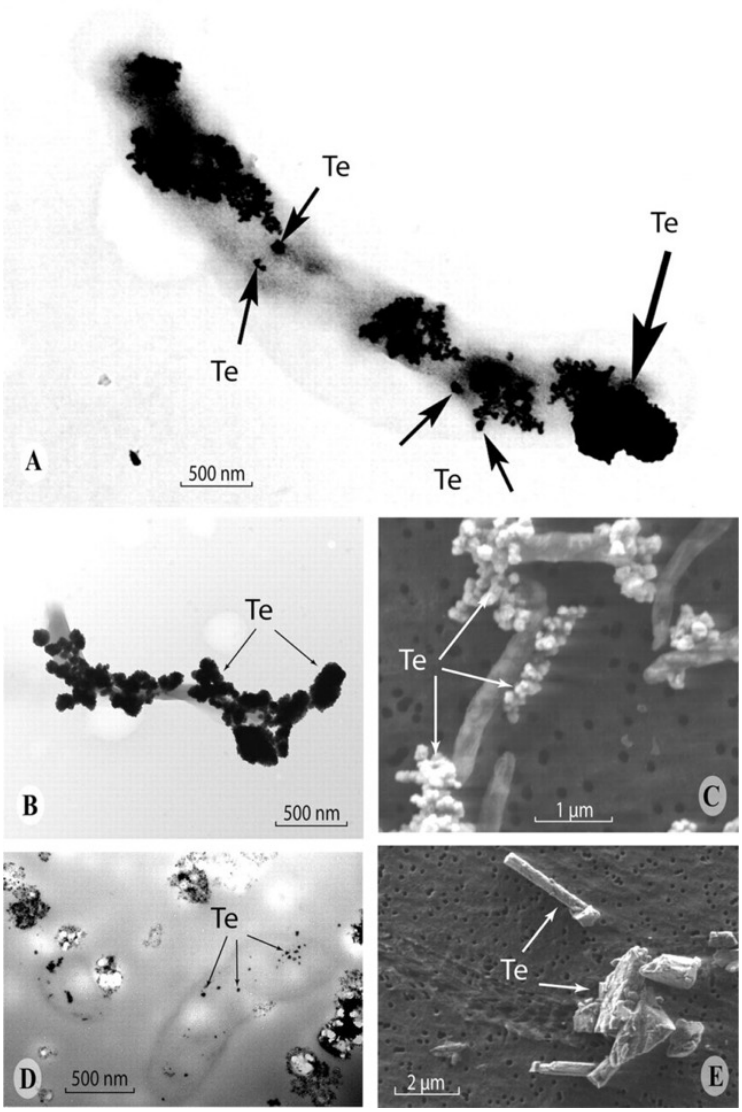

Formation of irregular Te(0) "nanospheres" by S. barnesii. (A) Whole-mount TEM image of a single cell grown on Te(VI) showing abundant external Te nanospheres (small arrows) forming larger aggregates (large arrow) on the cell surfaces. (B) Lower-magnification TEM image of another single cell grown on Te(VI) showing abundant external Te nanospheres. (C) Wide-field SEM image of the Te(0) nanosphere aggregates formed after growth on Te(VI). (D) Unstained TEM thin-section image of cells grown on Te(VI) showing internal accumulations of Te(0). (E) SEM image of Te(0) obtained from a chemical supply house.

Over the last decade, sol-gel derived Ormosil ceramics have emerged as an archetypal candidate for transparent, robust, tailorable host-matrix materials in the fields of high-performance

optics, nonlinear optics, and optoelectronics.[7, 99-105] In distinction to organic polymers, Ormosil ceramics characteristically exhibit excellent thermal and mechanical stability, compositional homogeneity, and desirable baseline optical properties (e.g., high-transparencies/tunable refractive indices). Such properties are tailorable via modification of the sol precursor(s), solvent(s), catalyst(s), additive(s), water content, reaction conditions (e.g., pH, temperature, pressure, and time), and gelation/densification conditions, owing largely to the facile nature of the sol-gel process.[98] Regarding formability, the dynamic reaction kinetics of the gelation process in the preparation of sol-gel derived Ormosil ceramics allows gels to be molded/cast into lenses/monolithic optical components, drawn into optical fibers, or printed in 2D/3D onto application-specific substrates to form patterned thin-films, optical waveguides, and optical resonators. This work reports on both the linear and nonlinear optical properties of Te^0 harvested from the anaerobe *Bacillus Selenitireducens* (bio-Te^0) immobilized within monolithic transparent solid-state Ormosil matrices. Comparisons to chemically synthesized Te^0 are investigated and potential optical limiting and nonlinear optical applications are discussed.

The response of an optical medium to the incident electromagnetic field is the induced dipole moments in the medium. Dipole moment per unit volume is Polarization,

$$\boldsymbol{Pi} = P_i^0 + \chi_{ij}\,\boldsymbol{Ej} \text{ (linear)}$$

where P_i^0 is permanent polarization; it is zero except for ferroelectric materials. *P*i is induced polarization, χ ij is the electric susceptibility tensor. At high intensity, polarization become nonlinear.

$$\boldsymbol{Pi} = \boldsymbol{\chi_{ij}}^{(1)}\,Ej + \boldsymbol{\chi_{ijk}}^{(2)}\,Ej{\cdot}Ek + \boldsymbol{\chi_{ijkl}}^{(3)}\,Ei{\cdot}Ej{\cdot}Ek + \ldots$$

$= P(1) + P(2) + P(3) + \ldots\chi(n)$ are higher order susceptibilities, and become $(n + 1)$ rank tensor.

The potential of these systems also optical non-linearities that are complete in the solid state and no longer dependent on liquid state conditions.

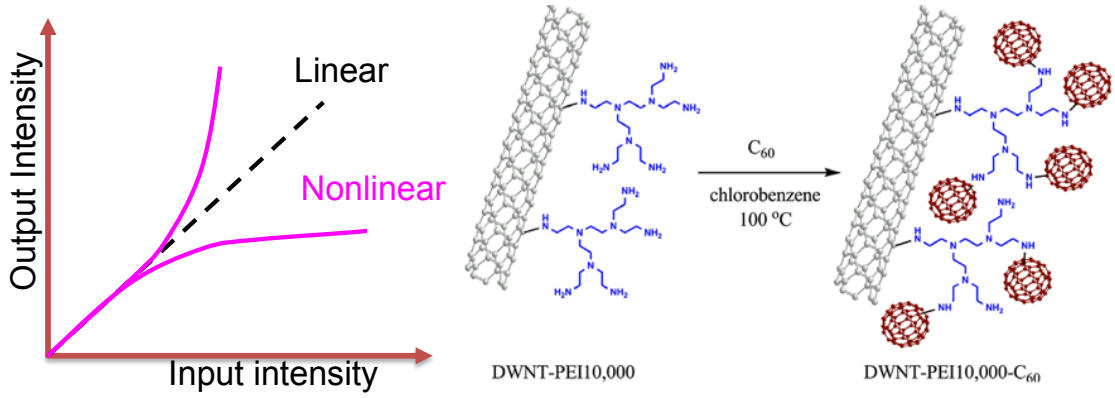

This is third order NLO process that requires three photons (ω1) in order to generate one photon of tripled frequency (3ω1). Non-centrosymmetric structure is not necessary for THG, as in SHG. Usually nanostructures are the THG enhancing agents. X (3) are expected to play a key role in optical switching devices since their optical properties can be controlled by light. However, due to some high order of nonlinearity these materials are usually less efficient and have not reached the maturity of $\chi(2)$ materials for device applications.

Conclusion and Future

The overarching aims and objectives of this paper can be holistically partitioned into four distinct parts as follows: by addressing methods by which scalable MWCNT-based DCPNs are formed through percolating random networks of MWCNTs using nondestructive synthesis techniques. A description of a facile nanocomposite surface silanization technique that effectively mitigates the detrimental effects of water ingress from environmental conditions that such materials are expected to perform under. An investigation of an alternative approach towards improving the repeatability/reversibility, electrical/thermal conductance, and thermoresponsivity of MWCNT-based DCPNs near hyperpyrexia temperatures *via* tailored covalent modification of the filler/host-matrix interface/interphase, effectuated across form-stable 2nd-order glass transitions. Finally, there is a whole wealth of optical and nonlinear optical properties of sol-gel derived monolithic, transparent, Ormosil-

based, ceramic nanocomposites of functionalized bio-Te^0 synthesized by the anaerobe *Bacillus Selenitireducens*.

However, rather than using a singularly synthesized material, it would make more sense to do so using suitable hosts and fillers, while we will see on the increase since we published solid state switching in Nature Communications 2019 or similar properties that include Phthalocyanines, porphyrins, fullerenes, nanotubes, graphene and even bacterially produced rare earths.

References

[1] Shaffer, G. D. (**1993**). An archaeomagnetic study of a wattle and daub building collapse. *Journal of Field Archaeology*, *20*(1), 59-75.

[2] Ma, P.-C., Siddiqui, N. A., Marom, G., & Kim, J.-K. (**2010**). Dispersion and functionalization of carbon nanotubes for polymer-based nanocomposites: a review. *Composites Part A: Applied Science and Manufacturing*, *41*(10), 1345-1367.

[3] Mack, H. (**2004**). Silane oligomers: a class of their own. *Silanes and Other Coupling Agents*, *3*(1), 11-20.

[4] Pohl, E., Chaves, A., Danahey, C., Sussman, A., & Bennett, V. (**2000**). Sterically hindered silanes for waterborne systems: a model study of silane hydrolysis. *Silanes and Other Coupling Agents*, *2*, 15-25.

[5] Maharjan, S., Liao, K.-S., Wang, A. J., Barton, K., Haldar, A., Alley, N. J., Byrne, H. J., & Curran, S. A. (**2020**). Self-cleaning hydrophobic nanocoating on glass: A scalable manufacturing process. *Materials Chemistry and Physics*, *239*, 122000.

[6] Jin, M., Wang, J., Yao, X., Liao, M., Zhao, Y., & Jiang, L. (**2011**). Underwater Oil Capture by a Three-Dimensional Network Architectured Organosilane Surface. *Advanced Materials*, *23*(25), 2861-2864.

[7] Maharjan, S., Liao, K.-S., Wang, A. J., Zhu, Z., Alam, K., McElhenny, B. P., Bao, J., & Curran, S. A. (**2019**). Functionalized few-layered graphene oxide embedded in an organosiloxane matrix for applications in optical limiting. *Chemical Physics Letters*, *714*, 149-155.

[8] Maharjan, S., Liao, K.-S., Wang, A. J., Zhu, Z., McElhenny, B. P., Bao, J., & Curran, S. A. (**2019**). Synthesis of Stabilized Silver Nanoparticles in Organosiloxane Matrix via Sol-Gel Method and its Optical Nonlinearity Study. *Chemical Physics*, 110610.

[9] Shim, M., Javey, A., Shi Kam, N. W., & Dai, H. (**2001**). Polymer functionalization for air-stable n-type carbon nanotube field-effect transistors. *Journal of the American Chemical Society*, *123*(46), 11512-11513.

[10] Kim, S. H., Song, W., Jung, M. W., Kang, M. A., Kim, K., Chang, S. J., Lee, S. S., Lim, J., Hwang, J., & Myung, S. (**2014**). Carbon nanotube and graphene hybrid thin film for transparent electrodes and field effect transistors. *Advanced Materials*, *26*(25), 4247-4252.

[11] Yamada, T., Hayamizu, Y., Yamamoto, Y., Yomogida, Y., Izadi-Najafabadi, A., Futaba, D. N., & Hata, K. (**2011**). A stretchable carbon nanotube strain sensor for human-motion detection. *Nature Nanotechnology*, *6*(5), 296.

[12] Zhang, J., Wang, R., Zhu, X., Pan, A., Han, C., Li, X., Dan, Z., Ma, C., Wang, W., Su, H., & Niu, C. (**2017**). Pseudo-topotactic conversion of carbon nanotubes to T-carbon nanowires under picosecond laser irradiation in methanol. *Nature Communications*, *8*(1), 683.

[13] Sheng, X.-L., Yan, Q.-B., Ye, F., Zheng, Q.-R., & Su, G. (**2011**). T-carbon: a novel carbon allotrope. *Physical Review Letters*, *106*(15), 155703.

[14] Jo, J. Y., & Kim, B. G. (**2012**). Carbon allotropes with triple bond predicted by first-principle calculation: Triple bond modified diamond and T-carbon. *Physical Review B*, *86*(7), 075151.

[15] Kim, H., Abdala, A. A., & Macosko, C. W. (**2010**). Graphene/polymer nanocomposites. *Macromolecules*, *43*(16), 6515-6530.

[16] Allen, M. J., Tung, V. C., & Kaner, R. B. (**2009**). Honeycomb carbon: a review of graphene. *Chemical Reviews*, *110*(1), 132-145.

[17] Diankov, G., Neumann, M., & Goldhaber-Gordon, D. (**2013**). Extreme monolayer-selectivity of hydrogen-plasma reactions with graphene. *ACS Nano*, *7*(2), 1324-1332.

[18] Li, Y., Yuan, H., Von Dem Bussche, A., Creighton, M., Hurt, R. H., Kane, A. B., & Gao, H. (**2013**). Graphene microsheets enter cells through spontaneous membrane penetration at edge asperities and corner sites. *Proceedings of the National Academy of Sciences*, *110*(30), 12295-12300.

[19] Iijima, S. (**1991**). Helical microtubules of graphitic carbon. *Nature*, *354*(6348), 56.

[20] Chen, J., Liu, B., Gao, X., & Xu, D. (**2018**). A review of the interfacial characteristics of polymer nanocomposites containing carbon nanotubes. *RSC Advances*, *8*(49), 28048-28085.

[21] Jung, Y. J., Kar, S., Talapatra, S., Soldano, C., Viswanathan, G., Li, X., Yao, Z., Ou, F. S., Avadhanula, A., Vajtai, R., Curran, S., Nalamasu, O., & Ajayan, P. M. (**2006**). Aligned Carbon Nanotube−Polymer Hybrid Architectures for Diverse Flexible Electronic Applications. *Nano Letters*, *6*(3), 413-418.

[22] Ajayan, P., Stephan, O., Colliex, C., & Trauth, D. (**1994**). Aligned carbon nanotube arrays formed by cutting a polymer resin---nanotube composite. *Science*, *265*(5176), 1212-1214.

[23] Wei, C., Dai, L., Roy, A., & Tolle, T. B. (**2006**). Multifunctional chemical vapor sensors of aligned carbon nanotube and polymer composites. *Journal of the American Chemical Society*, *128*(5), 1412-1413.

[24] Kinloch, I. A., Suhr, J., Lou, J., Young, R. J., & Ajayan, P. M. (**2018**). Composites with carbon nanotubes and graphene: An outlook. *Science*, *362*(6414), 547-553.

[25] Lee, S. W., Yabuuchi, N., Gallant, B. M., Chen, S., Kim, B.-S., Hammond, P. T., & Shao-Horn, Y. (**2010**). High-power lithium batteries from functionalized carbon-nanotube electrodes. *Nature Nanotechnology*, *5*(7), 531.

[26] Kim, H., Kim, K., Lee, C., Joo, J., Cho, S., Yoon, H., Pejaković, D., Yoo, J.-W., & Epstein, A. (**2004**). Electrical conductivity and electromagnetic interference shielding of multiwalled carbon nanotube composites containing Fe catalyst. *Applied Physics Letters*, *84*(4), 589-591.

[27] Munir, A. (**2017**). Microwave radar absorbing properties of multiwalled carbon nanotubes polymer composites: a review. *Advances in Polymer Technology*, *36*(3), 362-370.

[28] Liao, K.-S., Talla, J. A., Yambem, S. D., Birx, D., Chen, G., Coldren, F., Carroll, D. L., Ci, L., Ajayan, P. M., & Zhang, D. (**2010**). Formation of highly conductive composite coatings and their applications to broadband antennas and mechanical transducers. *Journal of Materials Research*, *25*(9), 1741-1747.

[29] Yang, Z., Chen, T., He, R., Guan, G., Li, H., Qiu, L., & Peng, H. (**2011**). Aligned carbon nanotube sheets for the electrodes of organic solar cells. *Advanced Materials*, *23*(45), 5436-5439.

[30] Sangermano, M., Pegel, S., Pötschke, P., & Voit, B. (**2008**). Antistatic epoxy coatings with carbon nanotubes obtained by cationic photopolymerization. *Macromolecular Rapid Communications*, *29*(5), 396-400.

[31] Liew, K., Lei, Z., & Zhang, L. (**2015**). Mechanical analysis of functionally graded carbon nanotube reinforced composites: a review. *Composite Structures*, *120*, 90-97.

[32] Rizzuto, C., Pugliese, G., Bahattab, M. A., Aljlil, S. A., Drioli, E., & Tocci, E. (**2018**). Multiwalled carbon nanotube membranes for water purification. *Separation and Purification Technology*, *193*, 378-385.

[33] Chandrabhas, N., Sood, A., Sundararaman, D., Raju, S., Raghunathan, V., Rao, G., Sastry, V., Radhakrishnan, T., Hariharan, Y., & Bharathi, A. (**1994**). Structure and vibrational properties of carbon tubules. *Pramana*, *42*(5), 375-385.

[34] Li, H. J., Lu, W., Li, J., Bai, X., & Gu, C. (**2005**). Multichannel ballistic transport in multiwall carbon nanotubes. *Physical Review Letters*, *95*(8), 086601.

[35] Gong, S., Zhu, Z., & Haddad, E. (**2013**). Modeling electrical conductivity of nanocomposites by considering carbon nanotube deformation at nanotube junctions. *Journal of Applied Physics*, *114*(7), 074303.

[36] Wang, Y., Weng, G. J., Meguid, S. A., & Hamouda, A. M. (**2014**). A continuum model with a percolation threshold and tunneling-assisted interfacial conductivity for carbon nanotube-based nanocomposites. *Journal of Applied Physics*, *115*(19), 193706.

[37] Haynes, W. M. (**2016**). *CRC Handbook of Chemistry and Physics*. CRC Press.

[38] Davis, E. (**1970**). Optical absorption, transport and photoconductivity in amorphous selenium. *Journal of Non-Crystalline Solids*, *4*, 107-116.

[39] Dou, L., Chang, W. H., Gao, J., Chen, C. C., You, J., & Yang, Y. (**2013**). A selenium-substituted low-bandgap polymer with versatile photovoltaic applications. *Advanced Materials*, *25*(6), 825-831.

[40] Xu, W., Song, J., Sun, L., Yang, J., Hu, W., Ji, Z., & Yu, S. H. (**2008**). Structural, Electrical, and Photoconductive Properties of Individual Single-Crystalline Tellurium Nanotubes Synthesized by a Chemical Route: Doping Effects on Electrical Structure. *Small*, *4*(7), 888-893.

[41] Gao, M., Kirstein, S., Möhwald, H., Rogach, A. L., Kornowski, A., Eychmüller, A., & Weller, H. (**1998**). Strongly photoluminescent CdTe nanocrystals by proper surface modification. *The Journal of Physical Chemistry B*, *102*(43), 8360-8363.

[42] Murray, C., Norris, D. J., & Bawendi, M. G. (**1993**). Synthesis and characterization of nearly monodisperse CdE (E= sulfur, selenium, tellurium) semiconductor nanocrystallites. *Journal of the American Chemical Society*, *115*(19), 8706-8715.

[43] Chivers, T., & Laitinen, R. S. (**2015**). Tellurium: a maverick among the chalcogens. *Chemical Society Reviews*, *44*(7), 1725-1739.

[44] Horike, S., Shimomura, S., & Kitagawa, S. (**2009**). Soft porous crystals. *Nature Chemistry*, *1*(9), 695.

[45] Zhu, Z., Cai, X., Yi, S., Chen, J., Dai, Y., Niu, C., Guo, Z., Xie, M., Liu, F., & Cho, J.-H. (**2017**). Multivalency-driven formation of Te-based monolayer materials: a combined first-principles and experimental study. *Physical Review Letters*, *119*(10), 106101.

[46] Reed, E. J. (**2017**). Two-dimensional tellurium. *Nature*, *552*(7683), 40.

[47] Guo, J., Zhao, J., Huang, D., Wang, Y., Zhang, F., Ge, Y., Song, Y., Xing, C., Fan, D., & Zhang, H. (**2019**). Two-dimensional tellurium--polymer membrane for ultrafast photonics. *Nanoscale*, *11*(13), 6235-6242.

[48] Liang, Z., Wang, Y., Hua, C., Xiao, C., Chen, M., Jiang, Z., Tai, R., Lu, Y., & Song, F. (**2019**). Electronic structures of ultra-thin tellurium nanoribbons. *Nanoscale*, *11*(30), 14134-14140.

[49] Zhou, G., Addou, R., Wang, Q., Honari, S., Cormier, C. R., Cheng, L., Yue, R., Smyth, C. M., Laturia, A., Kim, J., Vandenberghe, W. G., Kim, M. J., Wallace, R. M., & Hinkle, C. L. (**2018**). High-Mobility Helical Tellurium Field-Effect Transistors Enabled by Transfer-Free, Low-Temperature Direct Growth. *Advanced Materials*, *30*(36), 1803109.

[50] Du, Y., Qiu, G., Wang, Y., Si, M., Xu, X., Wu, W., & Ye, P. D. (**2017**). One-Dimensional van der Waals Material Tellurium: Raman Spectroscopy under Strain and Magneto-Transport. *Nano Letters*, *17*(6), 3965-3973.

[51] Kim, M.-S., Ma, X.-H., Cho, K.-H., Jeon, S.-Y., Hur, K., & Sung, Y.-M. (**2018**). A Generalized Crystallographic Description of All Tellurium Nanostructures. *Advanced Materials*, *30*(6), 1702701.

[52] Epstein, A., Fritzsche, H., & Lark-Horovitz, K. (**1957**). Electrical properties of tellurium at the melting point and in the liquid state. *Physical Review*, *107*(2), 412.

[53] Martin, R. M., Lucovsky, G., & Helliwell, K. (**1976**). Intermolecular bonding and lattice dynamics of Se and Te. *Physical Review B*, *13*(4), 1383.

[54] Lee, T. I., Lee, S., Lee, E., Sohn, S., Lee, Y., Lee, S., Moon, G., Kim, D., Kim, Y. S., & Myoung, J. M. (**2013**). High-Power Density Piezoelectric Energy Harvesting Using Radially Strained Ultrathin Trigonal Tellurium Nanowire Assembly. *Advanced Materials*, *25*(21), 2920-2925.

[55] Agapito, L. A., Kioussis, N., Goddard III, W. A., & Ong, N. P. (**2013**). Novel family of chiral-based topological insulators: elemental tellurium under strain. *Physical Review Letters*, *110*(17), 176401.

[56] Hirayama, M., Okugawa, R., Ishibashi, S., Murakami, S., & Miyake, T. (**2015**). Weyl node and spin texture in trigonal tellurium and selenium. *Physical Review Letters*, *114*(20), 206401.

[57] Ireland, R. M., Zhang, L., Gopalan, P., & Katz, H. E. (**2013**). Tellurium Thin Films in Hybrid Organic Electronics: Morphology and Mobility. *Advanced Materials*, *25*(31), 4358-4364.

[58] Wang, Y., Xiao, C., Chen, M., Hua, C., Zou, J., Wu, C., Jiang, J., Yang, S. A., Lu, Y., & Ji, W. (**2018**). Two-dimensional ferroelectricity and switchable spin-textures in ultra-thin elemental Te multilayers. *Materials Horizons*, *5*(3), 521-528.

[59] Araki, K., & Tanaka, T. (**1972**). Piezoelectric and elastic properties of single crystalline Se-Te alloys. *Japanese Journal of Applied Physics*, *11*(4), 472.

[60] Caldwell, R. S., & Fan, H. (**1959**). Optical properties of tellurium and selenium. *Physical Review*, *114*(3), 664.

[61] Miura, N., & Tanaka, S. (**1968**). Fast photoconductivity of tellurium by CO2 laser radiation. *Applied Physics Letters*, *12*(11), 374-375.

[62] Liu, J.-W., Zhu, J.-H., Zhang, C.-L., Liang, H.-W., & Yu, S.-H. (**2010**). Mesostructured assemblies of ultrathin superlong tellurium nanowires and their photoconductivity. *Journal of the American Chemical Society*, *132*(26), 8945-8952.

[63] Hirai, H., Sekiguchi, H., Miyata, S., & Kobayashi, S. (**1987**). Tellurium thin-film transistor deposited on polyester film having plasma polymerized films on double-layered gate insulators. *Applied Physics Letters*, *50*(13), 818-820.

[64] Lin, S., Li, W., Chen, Z., Shen, J., Ge, B., & Pei, Y. (**2016**). Tellurium as a high-performance elemental thermoelectric. *Nature Communications*, *7*, 10287.

[65] Wu, W., Qiu, G., Wang, Y., Wang, R., & Ye, P. (**2018**). Tellurene: its physical properties, scalable nanomanufacturing, and device applications. *Chemical Society Reviews*, *47*(19), 7203-7212.

[66] Wang, K., Zhang, X., Kislyakov, I. M., Dong, N., Zhang, S., Wang, G., Fan, J., Zou, X., Du, J., Leng, Y., Zhao, Q., Wu, K., Chen, J., Baesman, S. M., Liao, K.-S., Maharjan, S., Zhang, H., Zhang, L., Curran, S. A., Oremland, R. S., Blau, W. J., & Wang, J. (**2019**). Bacterially synthesized tellurium nanostructures for broadband ultrafast nonlinear optical applications. *Nature Communications*, *10*(1), 3985.

[67] Boudebs, G., Cherukulappurath, S., Guignard, M., Troles, J., Smektala, F., & Sanchez, F. (**2004**). Experimental observation of higher order nonlinear absorption in tellurium based chalcogenide glasses. *Optics Communications*, *232*(1-6), 417-423.

[68] Sandeep, C. S., Samal, A., Pradeep, T., & Philip, R. (**2010**). Optical limiting properties of Te and Ag2Te nanowires. *Chemical Physics Letters*, *485*(4-6), 326-330.

[69] Wang, Y., Qiu, G., Wang, R., Huang, S., Wang, Q., Liu, Y., Du, Y., Goddard, W. A., Kim, M. J., & Xu, X. (**2018**). Field-effect transistors made from solution-grown two-dimensional tellurene. *Nature Electronics*, *1*(4), 228.

[70] Huang, X., Guan, J., Lin, Z., Liu, B., Xing, S., Wang, W., & Guo, J. (**2017**). Epitaxial growth and band structure of Te film on graphene. *Nano Letters*, *17*(8), 4619-4623.

[71] Zhu, Y. J., Wang, W. W., Qi, R. J., & Hu, X. L. (**2004**). Microwave-assisted synthesis of single-crystalline tellurium nanorods and nanowires in ionic liquids. *Angewandte Chemie International Edition*, *43*(11), 1410-1414.

[72] Ma, C., Yan, J., Huang, Y., Wang, C., & Yang, G. (**2018**). The optical duality of tellurium nanoparticles for broadband solar energy harvesting and efficient photothermal conversion. *Science Advances*, *4*(8), eaas9894.

[73] Kang, S., Dai, T., Ma, X., Dang, S., Li, H., Hu, P., Yu, F., Zhou, X., Wu, S., & Li, S. (**2019**). Broad spectral response of an individual tellurium nanobelt grown by molecular beam epitaxy. *Nanoscale*, *11*(4), 1879-1886.

[74] Xi, G., Peng, Y., Yu, W., & Qian, Y. (**2005**). Synthesis, Characterization, and Growth Mechanism of Tellurium Nanotubes. *Crystal Growth & Design*, *5*(1), 325-328.

[75] Amani, M., Tan, C., Zhang, G., Zhao, C., Bullock, J., Song, X., Kim, H., Shrestha, V. R., Gao, Y., Crozier, K. B., Scott, M., & Javey, A. (**2018**). Solution-Synthesized High-Mobility Tellurium Nanoflakes for Short-Wave Infrared Photodetectors. *ACS Nano*, *12*(7), 7253-7263.

[76] Mayers, B., & Xia, Y. (**2002**). Formation of Tellurium Nanotubes Through Concentration Depletion at the Surfaces of Seeds. *Advanced Materials*, *14*(4), 279-282.

[77] Yang, T., Ke, H., Wang, Q., Tang, Y. a., Deng, Y., Yang, H., Yang, X., Yang, P., Ling, D., Chen, C., Zhao, Y., Wu, H., & Chen, H. (**2017**). Bifunctional Tellurium Nanodots for Photo-Induced Synergistic Cancer Therapy. *ACS Nano*, *11*(10), 10012-10024.

[78] Li, G., Cui, X., Tan, C., & Lin, N. (**2014**). Solvothermal synthesis of polycrystalline tellurium nanoplates and their conversion into single crystalline nanorods. *RSC Advances*, *4*(2), 954-958.

[79] Medina Cruz, D., Tien-Street, W., Zhang, B., Huang, X., Vernet Crua, A., Nieto-Argüello, A., Cholula-Díaz, J. L., Martínez, L., Huttel, Y., González, M. U., García-Martín, J. M., & Webster, T. J. (**2019**). Citric juice-mediated synthesis of tellurium nanoparticles with antimicrobial and anticancer properties. *Green Chemistry*, *21*(8), 1982-1998.

[80] He, Z., Yang, Y., Liu, J.-W., & Yu, S.-H. (**2017**). Emerging tellurium nanostructures: controllable synthesis and their applications. *Chemical Society Reviews*, *46*(10), 2732-2753.

[81] Oremland, R. S., Herbel, M. J., Blum, J. S., Langley, S., Beveridge, T. J., Ajayan, P. M., Sutto, T., Ellis, A. V., & Curran, S. (**2004**). Structural and spectral features of selenium nanospheres produced by Se-respiring bacteria. *Applied and Environmental Microbiology*, *70*(1), 52-60.

[82] Oremland, R. S., Hollibaugh, J. T., Maest, A. S., Presser, T. S., Miller, L. G., & Culbertson, C. W. (**1989**). Selenate reduction to elemental selenium by anaerobic bacteria in sediments and culture: biogeochemical significance of a novel, sulfate-independent respiration. *Applied and Environmental Microbiology*, *55*(9), 2333-2343.

[83] Oremland, R. S., Blum, J. S., Culbertson, C. W., Visscher, P. T., Miller, L. G., Dowdle, P., & Strohmaier, F. E. (**1994**). Isolation, growth, and metabolism of an obligately anaerobic, selenate-respiring bacterium, strain SES-3. *Applied and Environmental Microbiology*, *60*(8), 3011-3019.

[84] Baesman, S. M., Bullen, T. D., Dewald, J., Zhang, D., Curran, S., Islam, F. S., Beveridge, T. J., & Oremland, R. S. (**2007**). Formation of tellurium nanocrystals during anaerobic growth of

bacteria that use Te oxyanions as respiratory electron acceptors. *Applied and Environmental Microbiology*, *73*(7), 2135-2143.

[85] Yurkov, V., Jappe, J., & Vermeglio, A. (**1996**). Tellurite resistance and reduction by obligately aerobic photosynthetic bacteria. *Applied and Environmental Microbiology*, *62*(11), 4195-4198.

[86] Blum, J. S., Bindi, A. B., Buzzelli, J., Stolz, J. F., & Oremland, R. S. (**1998**). Bacillus arsenicoselenatis, sp. nov., and Bacillus selenitireducens, sp. nov.: two haloalkaliphiles from Mono Lake, California that respire oxyanions of selenium and arsenic. *Archives of Microbiology*, *171*(1), 19-30.

[87] Baesman, S., Stolz, J., Kulp, T., & Oremland, R. S. (**2009**). Enrichment and isolation of Bacillus beveridgei sp. nov., a facultative anaerobic haloalkaliphile from Mono Lake, California, that respires oxyanions of tellurium, selenium, and arsenic. *Extremophiles*, *13*(4), 695-705.

[88] Xiong, L.-H., Cui, R., Zhang, Z.-L., Tu, J.-W., Shi, Y.-B., & Pang, D.-W. (**2015**). Harnessing Intracellular Biochemical Pathways for In Vitro Synthesis of Designer Tellurium Nanorods. *Small*, *11*(40), 5416-5422.

[89] Ramos-Ruiz, A., Field, J. A., Wilkening, J. V., & Sierra-Alvarez, R. (**2016**). Recovery of Elemental Tellurium Nanoparticles by the Reduction of Tellurium Oxyanions in a Methanogenic Microbial Consortium. *Environmental Science & Technology*, *50*(3), 1492-1500.

[90] Wang, X., Pu, J., An, B., Li, Y., Shang, Y., Ning, Z., Liu, Y., Ba, F., Zhang, J., & Zhong, C. (**2018**). Programming Cells for Dynamic Assembly of Inorganic Nano-Objects with Spatiotemporal Control. *Advanced Materials*, *30*(16), 1705968.

[91] Zonaro, E., Lampis, S., Turner, R. J., Qazi, S. J. S., & Vallini, G. (**2015**). Biogenic selenium and tellurium nanoparticles synthesized by environmental microbial isolates efficaciously inhibit bacterial planktonic cultures and biofilms. *Frontiers in Microbiology*, *6*, 584.

[92] Zare, B., Faramarzi, M. A., Sepehrizadeh, Z., Shakibaie, M., Rezaie, S., & Shahverdi, A. R. (**2012**). Biosynthesis and recovery of rod-shaped tellurium nanoparticles and their bactericidal activities. *Materials Research Bulletin*, *47*(11), 3719-3725.

[93] Yang, H., Qi, D., Liu, Z., Chandran, B. K., Wang, T., Yu, J., & Chen, X. (**2016**). Soft thermal sensor with mechanical adaptability. *Advanced Materials*, *28*(41), 9175-9181.

[94] Chen, Z., Hsu, P.-C., Lopez, J., Li, Y., To, J. W., Liu, N., Wang, C., Andrews, S. C., Liu, J., & Cui, Y. (**2016**). Fast and reversible thermoresponsive polymer switching materials for safer batteries. *Nature Energy*, *1*(5), 15009.

[95] Briscoe, J., Jalali, N., Woolliams, P., Stewart, M., Weaver, P. M., Cain, M., & Dunn, S. (**2013**). Measurement techniques for piezoelectric nanogenerators. *Energy & Environmental Science*, *6*(10), 3035-3045.

[96] Chung, D., Kim, S., & Lee, S. (**2008**). Carbon materials for thermal management. *Carbon Letters*, *9*(4), 259-270.

[97] Liu, R., Zhang, Q., Zhang, S., Sun, H., Liu, Z., Song, P., & Wang, J. (**2018**). Facile preparation of ultralight reduced graphene oxide/cellulose aerogel and its application in dye removal. *Cellulose*, *25*(9), 4949-4958.

[98] Khan, N. A., Hasan, Z., & Jhung, S. H. (**2013**). Adsorptive removal of hazardous materials using metal-organic frameworks (MOFs): a review. *Journal of Hazardous Materials*, *244*, 444-456.

[99] Polarz, S., Orlov, A., Schüth, F., & Lu, A. H. (**2007**). Preparation of High-Surface-Area Micro- and Mesoporous Carbon Nitrides by Nanocasting Using Various Siliceous Matrices. *Chemistry - A European Journal*, *13*(2), 592-597.

[100] Lee, J., Kim, J., & Hyeon, T. (**2006**). Recent progress in the synthesis of porous carbon materials. *Advanced Materials*, *18*(16), 2073-2094.

[101] Kaneko, K., & Rodríguez-Reinoso, F. (**1997**). Nanoporous materials: synthesis and characterization. In *Studies in Surface Science and Catalysis* (Vol. 103, pp. 103-114). Elsevier.

[102] Deng, Y., Cai, Y., Sun, Z., Liu, J., Liu, C., Wei, J., Li, W., Liu, C., Wang, Y., & Zhao, D. (**2010**). Multifunctional mesoporous composite microspheres with well-designed nanostructure: a highly integrated catalyst system. *Journal of the American Chemical Society*, *132*(24), 8466-8473.

[103] Inagaki, M., Toyoda, M., Soneda, Y., Tsujimura, S., & Morishita, T. (**2016**). Templated mesoporous carbons: synthesis and applications. *Carbon*, *107*, 448-473.

[104] Mizoshita, N., Goto, Y., Tani, T., & Inagaki, S. (**2009**). Efficient photocatalytic degradation of trichloroethylene by periodic mesoporous organosilicas loaded with gold nanoparticles. *Langmuir*, *25*(13), 7345-7348.

[105] Zayat, M., Pardo, R., Castellón, E., Torres, L., Almendro, D., Alarcón, J., & Levy, D. (**2007**). Preventing environmental damage produced by cultural heritage conservation treatments: new nanomaterials. *Materials Research Society Symposium Proceedings*, *1047*, Y02-06.

[106] Liao, K.-S., Wang, K., Shu, J., Maharjan, S., Wang, A. J., Curran, S. A., & Oremland, R. S. (**2021**). Resolving Nanocomposite Interfaces via Simultaneous Thermogravimetric and Nano-Scale Infrared Spectroscopy. *Analytical Chemistry*, *93*(5), 2898-2905.

[107] Maharjan, S., Liao, K.-S., Wang, A. J., Curran, S. A., & Oremland, R. S. (**2019**). Sol-gel synthesis of stabilized silver nanoparticles in an organosiloxane matrix for optical limiting applications. *Chemical Physics*, *522*, 78-84.

[108] Liao, K.-S., Maharjan, S., Wang, A. J., Zhang, D., Oremland, R. S., & Curran, S. A. (**2018**). Poly(octadecyl acrylate)-Grafted Multiwalled Carbon Nanotube Nanocomposites for Applications in Thermally Responsive Coatings. *ACS Applied Nano Materials*, *1*(10), 5759-5768.